J Mater Sci (2009) 44:4511–4521
DOI 10.1007/s10853-009-3654-x

REVIEW

Application of scanning electrochemical microscope in the study of corrosion of metals

Lin Niu · Yuehua Yin · Weikuan Guo · Min Lu · Ruijie Qin · Shenhao Chen

Received: 9 January 2009 / Accepted: 1 June 2009 / Published online: 14 June 2009

Abstract Scanning electrochemical microscope (SECM) has become a very useful and powerful technique for probing a variety of electrochemical reactions in corrosion process due to its high spatial resolution and electrochemical sensitivity to characterize the topography and redox activities of the metal/electrolyte solution interface. Its capability for the direct identification of chemical species in localized corrosion processes with high spatial resolution would be more advantageous compared to other local probe techniques with only morphological characterization. In this review, the applications of the SECM in the study of early stages of localized corrosion, electroactive defect sites in passive films, local initiation of pits, degradation of coating properties on steels, and some combined methods through SECM integrated with other techniques have been summarized and commented. Finally, the optimization for SECM's experiment design and operation as well as foreseeable application range has been proposed.

Introduction

Corrosion is the destructive attack of a material by reaction with its environment. The serious consequences of the corrosion process have become a problem of worldwide significance. In addition to our everyday encounters with this form of degradation, corrosion causes plant shutdowns, waste of valuable resources, loss or contamination of product, reduction in efficiency, costly maintenance, and expensive over design. It can also jeopardize safety and inhibit technological progress.

As one of the two types of corrosion, generalized corrosion processes that take place on metals are usually correlated with uniform metallic reactivity, with low or controlled reaction rates allowing life prediction of materials. To study generalized corrosion phenomena, conventional electrochemical techniques such as steady-state polarization curves and electrochemical impedance spectroscopy (EIS) [1–4] have been widely used to provide important information about the global properties of the metal/electrolyte solution interface and its large-scale corrosion activity. However, macroscopic symptoms of corrosion are only an expression of the final stages of a complex, dynamic sequence that starts at the microscopic level and do not offer much detailed information about the localized dynamics of corrosion processes [5].

Conversely, localized corrosion of passive metals such as pitting corrosion occurs on discrete locations. In these cases, the local metal dissolution leads to the formation of small active areas (i.e., microscopic defects such as pits, cracks, pores, etc.) within the passive surface area of the metal forming a heterogeneous electrode [6]. This kind of corrosion remains difficult to foresee and can propagate in depth in the bulk material depending on the nature of the species in solution.

To characterize localized processes occurred in corrosion of various metals, during the past decade, several local electrochemical measurement techniques, including scanning reference electrode technique (SRET) [7–9], scanning vibrating electrode technique (SVET) [7, 10–12], local

L. Niu (✉) · Y. Yin · W. Guo · M. Lu · R. Qin · S. Chen
School of Chemistry and Chemical Engineering, Shandong University, Jinan 250100, China
e-mail: lniu@sdu.edu.cn; niulin80@yahoo.com.cn

S. Chen
Institute of Metal Research, Chinese Academy of Sciences, Shenyang 110016, China

electrochemical impedance spectrum (LEIS) [7, 13, 14], scanning Kelvin probe (SKP) [7, 15], electrochemical microcell technique [7, 16], and SECM, have been successfully utilized and developed. Although the SRET and SVET, measuring potential distributions and current densities, respectively, near corrosion sites, have been used prior to the SECM for examination of corrosion processes, they do not directly provide any chemical information. In comparison, the SECM, pioneered by Engstrom et al. [17] in 1986 for probing concentration profiles within the diffusion layer of electrodes with conventional dimensions and detecting short-life reaction intermediates, allows the micrometer range to be reached readily by using usual microdisk electrodes as probes. Moreover, the SECM appears most suitable due to its ability to analyze larger areas of the sample than other in situ methods and can be tuned for chemical specificity. Large area measurements are important because the microstructures of most samples of interest are heterogeneous with multiple phases present [18]. In a series of researches over 20 years, the SECM technique has been largely developed, and extended the ranges of application by Bard and co-workers [19–25].

Currently, the SECM has become a very powerful technique for probing a variety of electrochemical reactions owing to its high spatial resolution and electrochemical sensitivity to characterize the topography and redox activities of the metal/electrolyte interface [26–28]. Its capability for the direct identification of chemical species (e.g., corrosion products) in localized corrosion processes with high lateral resolution would be of great interest. In this article, some applications of the SECM in the study of early stages of localized corrosion, electroactive defect sites in passive films, local initiation of pits, degradation of coating properties on steels, and improvement in information acquisition through SECM integrated with other techniques have been summarized and reviewed as follows.

Identification of early stages of localized corrosion

The investigation of early stages of localized corrosion events is of great significance to deeply understand the initiation mechanisms of corrosion events. As well known, the nucleation stage is followed by a metastable stage in which propagation of the pit is not yet fully stabilized, but growth is sustained by the surrounding and covering geometry of the passive surface from which the pit began. This early stage of pit growth may be succeeded by the stable state, or growth may terminate while still in the metastable state [29]. The rate of growth is controlled by outward diffusion of metal cations from this saturated salt solution, the diffusion rate being sustained by the perforated remnants of the passive film that originally protected the site. Stable pit growth occurs when the pit depth alone provides the boundary depth necessary for diffusion control [30].

The electrochemistry of metastable pitting has been studied electrochemically by several groups [30–39]. The state is interesting because it is a precursor state to stable pitting and appears to be controlled by the same mechanism as that of stable pitting [30, 33]. Even in its metastable state of propagating pit on stainless steel, Fe^{2+} cations exude under diffusion control, the system becomes an ideal subject of study by SECM. Souto and co-workers presented the images describing metastable pits on 304 stainless steel obtained in situ in chloride solution at the open-circuit corrosion potential [29]. These images were obtained by SECM and represented the oxidation of Fe^{2+} emanating from the metastable pits as the probe tip passed over them. Each anodic transient on the tip was succeeded by a transient in the cathodic direction (Fig. 1). The authors ascribed this to an indirect observation of the cathodic reaction. It was shown that the lifetime of the detected pits was a maximum of a few seconds. In a following work, Souto and co-workers [40] demonstrated that mapping of concentration profiles of redox-active species participating in corrosion processes at the open-circuit potential can be performed with great accuracy and resolution using the scanning electrochemical microscope. This originated from the observation that the size of the microelectrode (tip) strongly determines the zone at which significant concentration gradients developed, thus expecting that the current detected at a micrometric probe will be indicative of true local concentration of a redox-active species being monitored [41].

Very small pulses in passive current density (pA scale) have been detected and assumed to represent "trigger events" for pitting corrosion [42]; an association with the nucleation of pitting corrosion has been demonstrated and some speculation has been made about the origin of these pulses [43, 44]. Zhu and Williams reported the SECM observation of a precursor state to pitting corrosion of stainless steel [37]. The objective of their work was to test the hypothesis that small-scale spatial and temporal fluctuations of passive current density of stainless steel in aqueous chloride media occur and to test whether pitting corrosion does arise as a consequence of the self-amplification of some such spatial fluctuations of passive current density. They presented the first results showing in some cases pitting arising from self-amplification of a local fluctuation, and demonstrated nucleation of a pit at a site marked by a marginally different passive current density to that pertaining on the rest of the surface.

Sulfur-rich inclusions in stainless steel (SS), e.g., MnS inclusions, are well known to serve as sites where corrosion pits form [45–49]. Ke and Alkire [50] used Auger electron spectroscopy (AES), scanning electron microscopy (SEM),

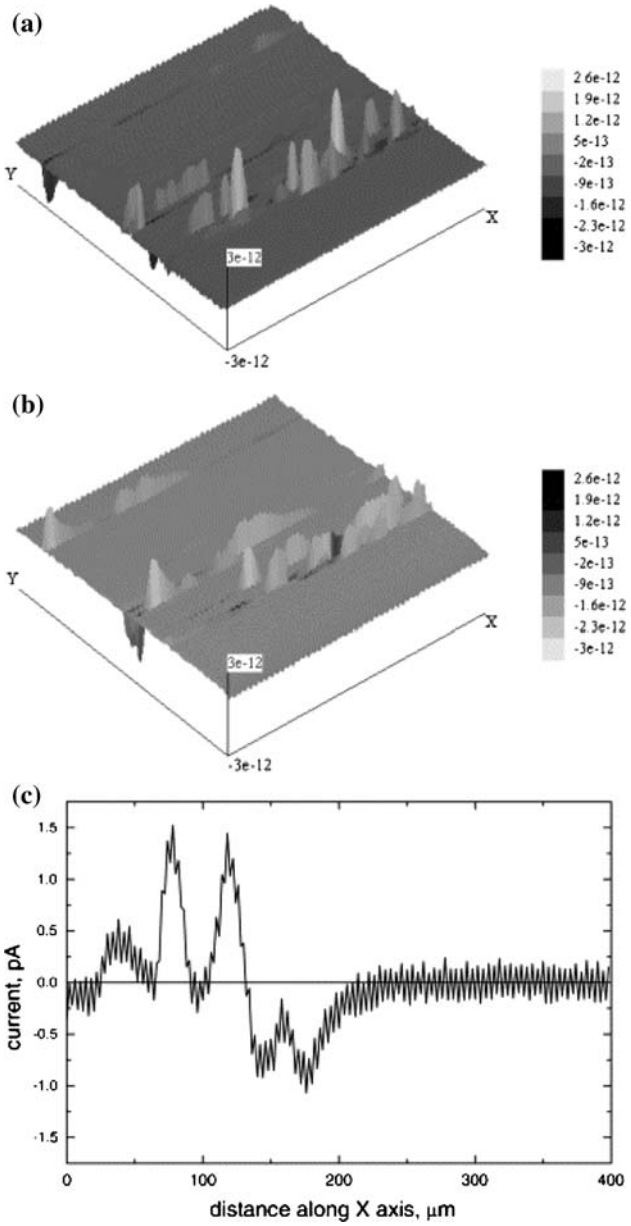

Fig. 1 SECM of stainless steel surface under immersion in 0.1 M HCl at the open-circuit corrosion potential. **a** The image as recorded, showing anodic peaks due to metastable pits. The upward direction in z is anodic. The x and y axes show an area 100 μm × 100 μm. The tip potential was 0.697 V (*SHE*). **b** The image in **a** turned upside down. In this image, the upward direction in z is cathodic. The tip potential was 0.697 V (*SHE*). **c** A line scan showing the positive (anodic) and negative (cathodic) wings of the tip current as it passes over a metastable pit and beyond. The tip potential was 0.997 V (*SHE*) (background rescaled to zero). Reprinted from [29]. Copyright 2004, Elsevier Science Ltd

and energy dispersive X-ray analysis (EDX) to study the onset of pitting on 304 SS in 0.1 M NaCl solution and reported that pits initiated only at MnS and mixed MnS/oxide inclusions with sizes above 0.7 μm. High concentrations of S were found within the pit cavity as well as the surrounding area. However, yet to be resolved was the mechanism for the specific chemical aspects of inclusion dissolution and how it led to acceleration of local metal dissolution, eventually to stable pitting corrosion [51]. Williams et al. have exploited the SECM to demonstrate states of metastable pitting on stainless steel when the alloy was polarized to high electrode potential, and have shown enhanced activity around the sites of sulfide inclusions. It was proposed that the conditions generated under the sulfur crust might be sufficiently extreme to cause the stainless steel to depassivate and a pit to trigger [38]. However, their work was carried out under potentiostatic control, instead of open circuit, which did not exactly match the conditions occurring in the majority of the practical corrosion situations, where a distribution of anodic and cathodic sites on the same corroding substrate existed.

To pursue further, it is of interest to probe the local chemistry involved with such high current flow, i.e., to measure the local distribution of dissolved sulfur species on a microscopic scale in the vicinity of a MnS inclusion during early stages of pit initiation. Paik et al. [51] studied the dissolution of MnS inclusions in 303 and 304 SS during initiation of pitting corrosion in an aqueous solution containing 10 mM KI and 0.1 M NaCl solutions by means of SECM technique. The dissolution products of MnS were detected amperometrically at a carbon fiber SECM tip using I^-/I_3^- as the redox mediator. SECM images showed that the sulfur species are slowly generated above previously identified MnS inclusions. SECM was found to be useful in mapping local concentration distributions of sulfur and their evolution in time during dissolution.

Lister and Pinhero extended the use of SECM for imaging localized sulfur concentrations dissolved from sulfide inclusions in type 304 SS. An unexpected current inversion at the microelectrode was observed at higher sample current densities in close proximity to the area where sulfur was detected at lower sample current. It was found that this inverted feature resulted from the localized increase in the electric field at the corrosion site, shifting the potential of the microelectrode when positioned over the site (Fig. 2). The work presented the first known combination of localized electric fields and chemical detection for determining localized electrochemical activity at a corroding surface [52]. Correlation of local electrochemical activity with areas of oxide breakdown has been made in some cases, thus suggesting that SECM could be used as a predictive tool to determine where corrosion might occur. As a sequent work to study the dynamics of localized corrosion, Lister and Pinhero probed local electrochemical activity of type 304 SS by using the I^-/I_3^- redox mediator in the substrate generation/tip collection mode (SG/TC) [53] of SECM. Imaging was performed over a large area with consecutive images of the same

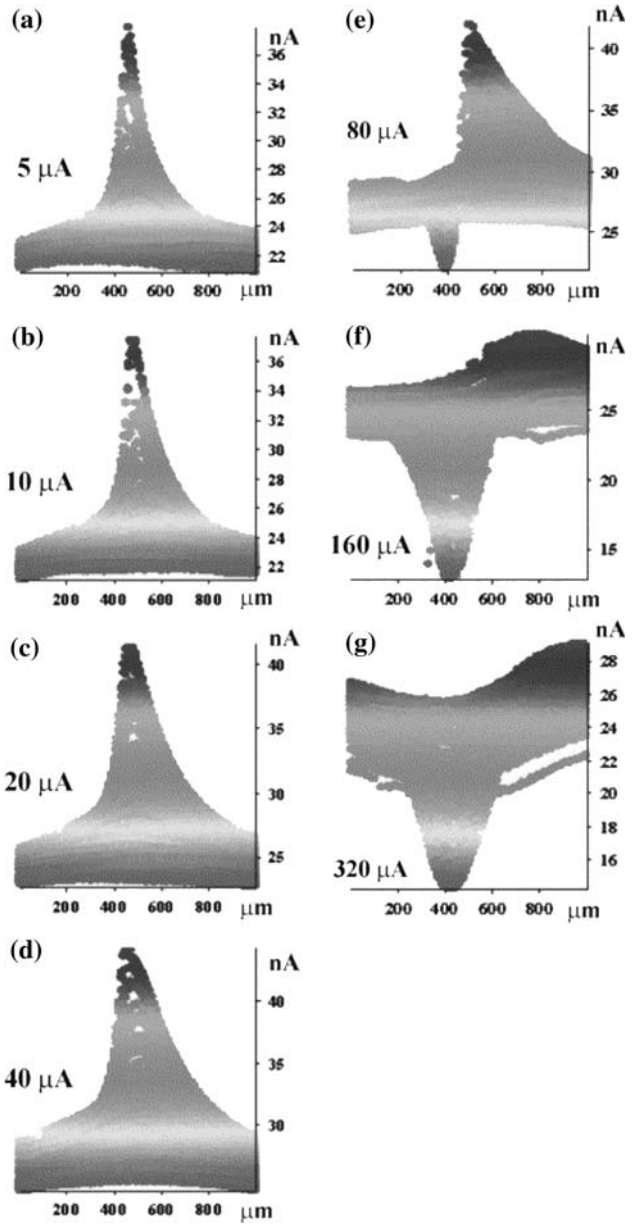

Fig. 2 Series of SECM images within the x–z plane taken over a dissolved sulfur inclusion peak at the following sample current densities: (**a**) 5; (**b**) 10; (**c**) 20; (**d**) 40; (**e**) 80; (**f**) 160; and (**g**) 320 μA. The microelectrode was held at 600 mV during the entire experiment. Reprinted from [52]. Copyright 2003, Elsevier Science Ltd

portion of the electrode captured. Localized active sites, which were determined to be corrosion processes, showed a time-dependent behavior when measured at a fixed potential. These results displayed pictures of the dynamic nature of corrosion and point to new ways of studying the fundamentals of pitting behavior [54]. As indicated by the authors, however, the technique was limited by the time required to raster a single probe through the scan area. A microelectrode array was proposed to obtain microscopic images with an improved temporal resolution in comparison with conventional SECM by avoiding the time-consuming scanning with an individual UME. It could be envisaged, however, that the lateral resolution will be much lower than in typical SECM images.

A direct identification of the chemical species with spatial resolution would be greatly advantageous. In the study of Völker et al. [55], local fluxes of ferrous ions at low-carbon steel surfaces coated with tin and an epoxy-phenolic resin on tinplate samples and at chrome steel (tin-free steel) have been monitored by oxidation of Fe^{2+} ions at a scanning Pt SECM tip. The SECM was employed in the collection mode at constant height on an x–y plane above the sample, monitoring the tip current as a function of tip location. Fushimi et al. [56] investigated the corrosion behavior of Fe-3 at.% Si alloy in 0.01 M HCl solution by using SECM as well as general electrochemistry. The SECM probe successively detected hydrogen in the vicinity of the corroding surface, imaged its distribution, and detected some active sites of the corroding surface. In the initial stage, a nonuniform distribution due to crystallographic orientation of substrate single grains was observed but soon diminished due to less activation of the corrosion reaction.

We have investigated the localized corrosion of type 304 stainless steel in neutral chloride solution by SECM area scan measurements [57]. Variations in the faradaic current measured at selected tip potential values can be related to changes in the local concentration and electrochemical activities of electroactive species involved in corrosion reactions occurring at the substrate as a function of immersion times of the substrate and polarizing currents or potentials applied on the substrate. To further verify the results acquired from cyclic voltammetric experiments, SECM measurements were employed to in situ study the compositions and electrochemical activity distribution profile of the pitting corrosion products of SS. It has been demonstrated that the combination of feedback current mode with generation-collection (G-C) mode of SECM is suitable to elucidate the possible reaction mechanisms and paths involved in the localized corrosion of stainless steel in neutral chloride solution.

Characterization of electroactive defect sites in passive films

Generally, there exists a thin passive layer (e.g., oxide film) on most of the surface of metal materials such as Al, Ti, Ta, Ni, etc. The integrity of the passive layer plays a key role in the protection of substrate metals. Identifying these structures in situ and demonstrating their relationship to localized corrosion is a challenging and important goal. In principle, SECM image allows in situ visualization of spatially localized electrochemical activity. A microscopic

redox-active site observed in an SECM image may reflect the higher electronic conductivity associated with a structural (or purely electronic) defect site in an otherwise passive oxide film (Fig. 3) [58]. Thus, SECM can provide key information on the local electronic properties of oxide films that are important in oxide film breakdown and localized corrosion. In previous studies, SECM has been used to study the localized electrochemical activity on Ti [59–61] and Ta [62] surfaces, primarily in nonaqueous media, covered by native and thick anodically grown oxide films of TiO_2 and Ta_2O_5, respectively. Oxide breakdown and pit nucleation at Ti/TiO_2 occur preferentially at defect sites where the localized electrochemical activity is largest [59, 60]. These SECM investigations provide a direct experimental demonstration of the relationship between electron transfer rates, oxide conductivity, and localized corrosion.

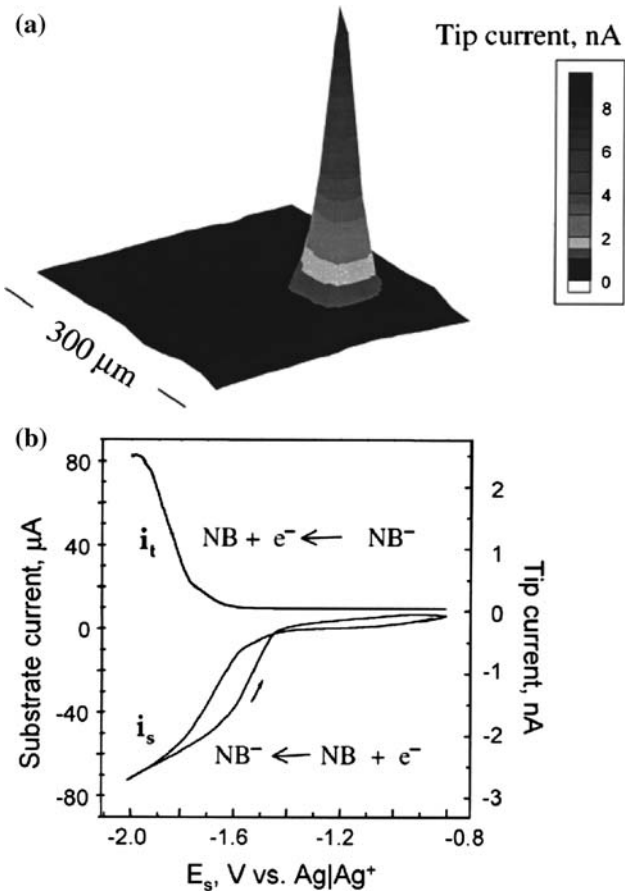

Fig. 3 **a** SECM image of an Al/Al_2O_3 electrode (99.9965% Al rod) rod surface showing a single electroactive site. The image was obtained by holding the Al/Al_2O_3 electrode at −1.7 V and the tip at 0.0 V vs. $Ag|Ag^+$. Tip was scanned at 5 µm/s during imaging. **b** Voltammetric response of the Al/Al_2O_3 electrode (i_s) and the corresponding tip response (i_t). The tip current was recorded by holding the tip potential, E_t, at 0.0 V while scanning the substrate potential (E_s). The tip was positioned directly above electroactive defect site at a separation of ~5 µm. Reprinted from [58]. Copyright 2003, The Electrochemical Society

Knowledge of the properties of the passive oxide layer on Al and its interaction with the environment (including hydration, anion adsorption/absorption, and chemical composition) is critical in developing a fundamental understanding of the mechanism of localized corrosion of this widely used material [58]. The oxide film on Al is known to contain microstructural and/or electronic defects that may be associated with local film breakdown. SECM also appeared well suited for investigations of the native oxide films on Al, which are 2–3 nm thick [63]. White and co-workers reported SECM studies of electroactive defect sites in the native oxide film on aluminum. Their results suggested that the oxide film contains highly conductive defect sites that are responsible for the observed electrochemical activity [58, 64]. It was focused on identifying the chemical and physical nature of these defect sites and determining their relationship to oxide film breakdown and localized corrosion.

Local induction or initiation of pits

Generally speaking, as pitting is a random event, it is difficult to predict where a pit will appear on the surface and how many pits will form. This renders difficult the use of local probes for studying the early stages of the pit initiation and propagation [6].

During the past few years, efforts have been made to initiate a single pit on a metal substrate [65–69]. In these cases, the pit generation at a predefined location was performed through the local supply in chloride ions in the vicinity of the metal surface. For instance, Still and Wipf [65] used SECM to induce localized corrosion at passivating iron surfaces by using the tip to generate Cl^- ions. The use of the SECM allowed the rapid establishment of a locally aggressive chemical environment at a preselected site on the iron surface. The susceptibility for passive layer breakdown and corrosion initiation was examined as a function of the time between the start of the passive layer growth and the formation of Cl^- ions. The breakdown of the passive layer was found to depend strongly on the passivation potential and the site of Cl^- formation on the iron surface. In addition to generating Cl^- ions, the SECM tip was simultaneously used to detect large iron ion concentration fluctuations as corrosion began. Current fluctuations at the tip were observed and ascribed to precursors to the passive layer breakdown. Fushimi and co-workers [66, 67, 69] reduced a silver chloride deposit at a silver microelectrode, resulting in local production of chloride ions close to the metal surface to initiate a single pit (Fig. 4). One of the main advantages of using the silver chloride microprobe is to have a reservoir of chloride ions

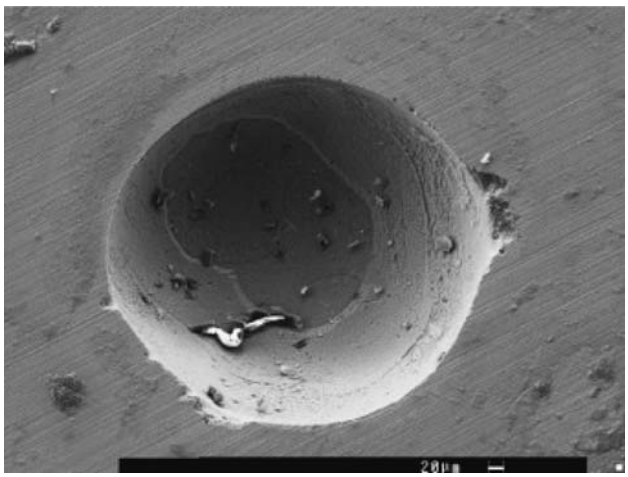

Fig. 4 SEM observation of a single pit generated on iron by SECM technique in 0.5 M H_2SO_4 solution. Reprinted from [6]. Copyright 2008, Elsevier Science Ltd

that can be released at a selected location without the adjunction of any other chemical.

As reported by Gabrielli et al. in [70, 71], the initiation and the propagation of a single pit on iron were controlled through the local production of chloride anion thanks to the silver chloride reduction at the tip of the SECM. The minimum amount of chloride ions to initiate a single pit was investigated as a function of the iron potential and the pH of the electrolytic solution. It was shown that the single pit propagation was associated with a parabolic increase of the amount of iron dissolved. The influence of the probe-to-substrate distance was also investigated. It was demonstrated that the use of the SECM to generate a single pit corresponded to a thin-layer configuration. The withdrawal of the Ag/AgCl microelectrode after the release of Cl^- ions evidenced that the pit propagation in full bath was much faster than in an electrolyte thin-layer-cell configuration.

Evaluation for degradation of coating properties on steels

Organic coatings are effectively utilized for the protection of metals due partly to their capacity to act as a physical barrier between the metal surface and corrosive environment in which they perform their function. However, all polymers are permeable to potentially corrosive species such as oxygen, water, and ions [72], which eventually lead to the initiation of metal corrosion under the polymeric film. In fact, defect-free films applied on metals are known to delaminate after some time, which indicates that species from the environment may diffuse either through microscopic pores in the coating or even through the polymer matrix [73]. However, the detailed mechanisms of the corrosion processes that take place at defect-free-coated metals, and of delamination in the vicinity of defects, are not yet fully understood. Although conventional electrochemical techniques such as EIS are capable of providing valuable information about these processes which are electrochemical in nature, they are integral and surface-averaged methods and thus lack spatial resolution, which is a major drawback especially in the early stages of the degradation process of coatings [74].

As one of the microelectrochemical measurement techniques to probe local electrochemical activity, the SECM has been utilized to study corrosion processes at coated metals. The mobile ultramicroelectrode immersed in an electrolyte solution was scanned in close proximity to the coating surface to characterize the topography and redox activity of the metal/coating interface with high spatial resolution. Application of the SECM to the study of the anticorrosive characteristics of the coated metals appeared to be very promising in elucidating the complex processes occurring in the interaction of the metal/coating system with corrosive environments [74]. Water uptake as well as swelling of the coating should be detectable because they resulted in a variation in the tip-sample separation. Such an effect would produce variations in the current flowing at the tip with time when the tip was scanned at a constant height from the sample (Fig. 5). In this area, Souto and co-workers have made a series of contributions [74–77]. For example, the damage to paint coatings caused by immersion in aqueous electrolyte solution has been observed in situ by SECM. The surface topography of coated metal samples as a function of time in chloride and sulfate solutions has been shown by SECM image. The degradation was observed as a swelling of the polyester coating as a function of time of immersion in chloride solution. The aggressive effect of chloride ions toward coating degradation was established after very short exposure times. In contrast, blistering could not be observed in a chloride-free sulfate solution [74]. In another work, Souto and co-workers demonstrated that SECM was suitable to investigate the processes involved in the degradation of coated metals. Both mapping of the surface and detection of reactants participating in the corrosion reactions were achieved by scanning the SECM-tip over the surface of the sample. This was possible because the SECM operated on both insulating (coated areas) and conducting (noncoated) surfaces and exhibited high spatial resolution. Furthermore, the SECM-tip may be used to quantitatively detect the reactants participating in the corrosion reactions by adequately calibrating the current measured at the tip in solutions of known concentration [75]. Also, SECM was employed to in situ monitor electroactive species in the proximity of a submillimeter defect (holiday) through the coating. Data obtained on the temporal variation of the current measured at the ultramicroelectrode when located in the proximity of the holiday will

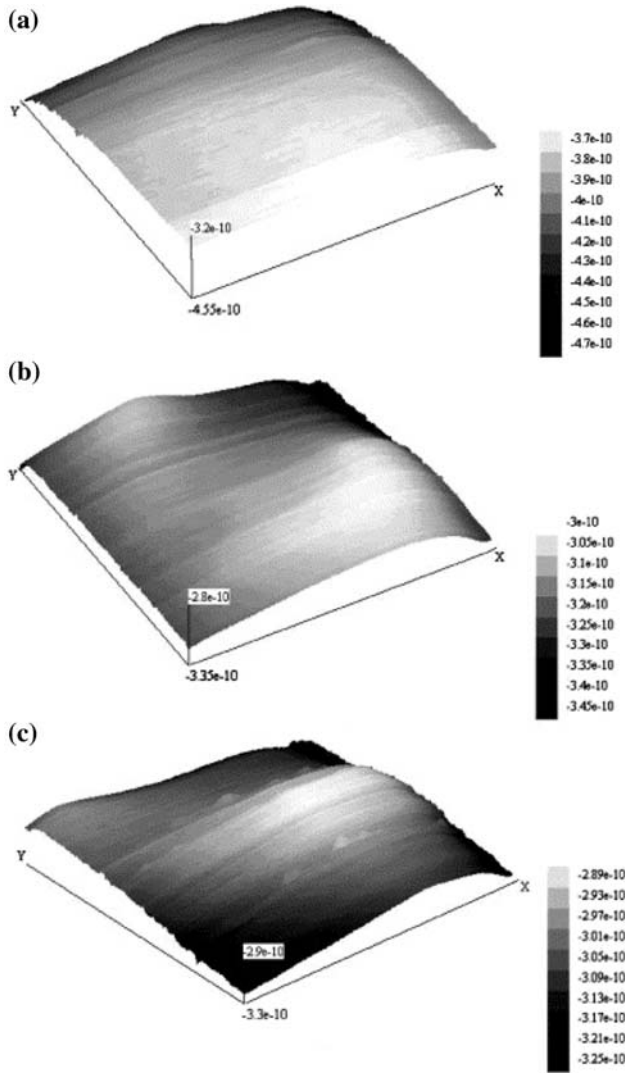

Fig. 5 Images generated by SECM of a painted specimen immersed in 0.1 M KCl solution. The image shown represent 100 μm × 100 μm in *X* and *Y* directions. The vertical *Z* direction is calibrated in terms of current at the tip. Tip potential, 0.5 V vs. the Ag/AgCl/KCl (saturated) reference electrode. The figures show a sequence taken at different times of the same surface: (**a**) immediately after immersion, (**b**) 21 min after immersion, and (**c**) 63 min after immersion. Times quoted represent the beginning of the scan; each scan lasted 20 min. Reprinted from [74]. Copyright 2004, Elsevier Science Ltd

be attributed to the corrosion processes at the metal–electrolyte interface. During these experiments, the SECM was operated alternatively in the SG-TC and the feedback modes in the same electrolyte solution under naturally occurring corrosion conditions [76]. As an attempt to evaluate the nature of metallic coating, Souto et al. focused on the investigation of the very early stages of the degradation of coil-coated galvanized steel sheet through swelling and blistering during exposure to chloride-containing aqueous solutions and the possible effect of the zinc-based metallic coating on the degradation at these very early stages [77]. SECM operating in the feedback mode was employed to image topographic changes when the samples were left at their spontaneous open circuit potential. Swelling of the coating and nucleation of blisters were observed for all the samples when they were exposed to naturally aerated 0.1 M KCl solution within 24 h exposure. It was found that the chloride ions promoted coating degradation nearly immediately upon immersion in the electrolyte with chloride concentrations of 0.1 M and above.

In addition, Katemann et al. used alternating current (AC) SECM to examine in situ the metal–coating interface of lacquered tinplates which are commonly used in industry to manufacture metal food containers [5]. It was demonstrated that AC-SECM allowed to visualize microscopic cracks and holes in the coating of the lacquered tinplates with high lateral resolution. As a matter of fact, these local defects in the corrosion-resistive tin/polymer coating were leading to an exposure of the underlying steel and had to be considered as potential precursor sites for localized corrosion.

Integrated with other techniques

In addition to SECM technique, there are other scanning probe techniques and microelectrochemical measurement techniques, with high spatial resolution and/or electrochemical activity probing capability, such as scanning tunneling microscopy (STM), atomic force microscopy (AFM), scanning Kelvin probe force microscopy (SKPFM), near-field scanning optical microscopy (NSOM), SVET, SRET, SKP, LEIS, etc. The combination of SECM with these techniques has been shown capable to provide microscopic information on the processes occurring at the surface of corroding metals.

Currently, strong efforts are under way to increase the resolution of SECM and to access the nanometer-size regime because many electrochemical phenomena are localized at much smaller structures [38, 78–81]. To allow SECM measurements in the nanometer dimension, a number of technical challenges have to be overcome. The combination of ECSTM with SECM allowed the collection of spatially correlated topographic and reactivity data (Fig. 6). With the topographic information obtained from the ECSTM experiment, a number of localized electrochemical experiments can be performed such as the recording of current–distance curves or two-dimensional SECM imaging in the nanometer-size regime [82].

Due to the complexity of the microstructure of multicomponent Al alloys, the mechanism of localized corrosion of Al alloys is still not completely understood, especially regarding the influence of various kinds of intermetallic precipitates in the alloys. As reported by Leygraf's group [83, 84], SECM has been integrated with electrochemical

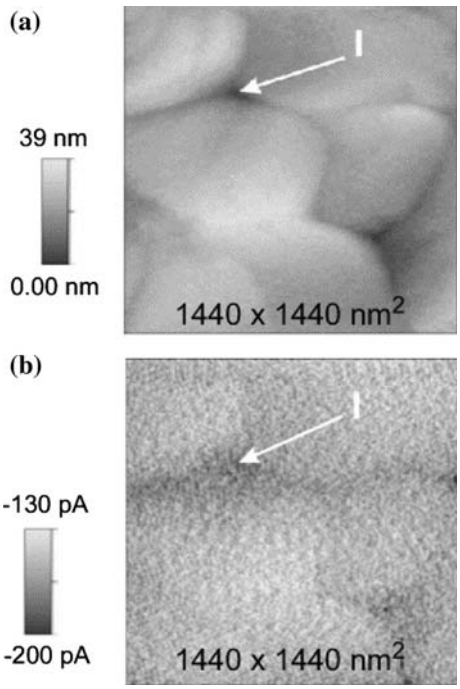

Fig. 6 Imaging of a bare gold surface in the combined ECSTM–SECM mode, image frame 1440 × 1440 nm^2. **a** ECSTM signal, $E_T = -50$ mV, $E_S = 0$ mV, tunneling current = 0.8 nA. **b** SECM signal, $E_T = -250$ mV, $E_S = 0$ mV, $r_{eff} = 72$ nm, $d = 20$ nm, solution 0.0052 M $[Ru(NH_3)_6]Cl_3$ + 0.1 M H_2SO_4, scan rate 6 μm/s. Reprinted from [82]. Copyright 2003, Elsevier Science Ltd

AFM (EC-AFM) and applied for in situ studies of the effect of intermetallic particles on localized corrosion of Al alloys in NaCl solution. Concurrent AFM topographic images and SECM electrochemical activity maps could be obtained in situ with micrometer lateral resolution, providing detailed information of the localized dissolution associated with different kinds of intermetallic particles, and deposition of corrosion products surrounding large particles or covering small pits. By using a dual-mode cantilever/tip, the AFM-based SECM had a high lateral resolution (better than normal SECM) and was able to reveal local dissolution sites. The critical issue in this approach is to fabricate a dual-mode cantilever/tip, which acted as the cantilever for the AFM and also the micro- or nanoelectrode tip for the SECM as well. To our knowledge, this is the first time the integrated EC-AFM/SECM was applied for in situ studies of localized corrosion of Al alloys.

Souto and co-workers [11] made use of the SECM and SVET to investigate microscopic aspects of the electrochemical reactions that occurred in an iron–zinc galvanic couple immersed in aqueous sodium chloride solution. The two techniques offered complementary information: ionic fluxes corresponding to cathodic and anodic reactions were measured with the SVET, though it lacked chemical discrimination to identify the nature of the ionic species involved; on the other hand, by adequately selecting the potential value at the microelectrode in the SECM, reactants and products of the corrosion reactions could be identified. Furthermore, their concentrations in the aqueous phase could be estimated, thus providing in situ information as a function of the time elapsed since immersion. It concluded that the two techniques had comparable sensitivity for the corrosion of iron, but significant differences were observed concerning the detection of corrosion of zinc.

The mechanism of protection of an aluminum substrate by a Mg-rich coating was also investigated using the combination of SECM with SVET [85]. The SVET has shown the evolution of the pit activity with time under sacrificial protection, whereas the SECM allowed indirect sensing of the cathodic activity above the electrodes. The results showed that the magnesium acted in a first stage by both preventing nucleation of pits and inhibiting the growth of the already existing ones, whereas at a later stage the precipitation of a porous layer of magnesium oxide at defective areas led to some degree of barrier protection.

NSOM, using tuning-fork control and specially fabricated tips to obtain high-resolution topography, has been used in combination with fluorescence microscopy and SECM to study localized corrosion behavior of AA2024 [86, 87]. The anodic dissolution sites were identified by the fluorescent dye, and ring-like deposition of corrosion products (aluminum oxyhydroxides) around intermetallic particles was observed both at open-circuit potential and under anodic polarization.

Another significant technique is the electrochemical quartz crystal microbalance (EQCM), which allows mass variations of the nanogramme order to be detected on surfaces of a few square millimeters [88]. The SECM–EQCM coupling allowed the simultaneous measurements of potential, current, and mass variations to be performed. The initiation and the propagation of a single pit on iron were controlled through the local production of chloride anion thanks to the silver chloride reduction at the tip of the SECM. The frequency variations, i.e., the mass variations, over the total QCM electrode can be related to a local event, and the frequency variations observed during the pit formation and propagation could be directly linked to the breakdown of the passive layer and to the dissolution of iron into Fe(II) in solution (Fig. 7) [70, 71]. One of the principal difficulties of this coupling is the radial dependence of the sensitivity of the EQCM.

AC-SECM combines electrochemical impedance measurements with SECM, which is a novel tool for measuring local interfacial impedance properties with high lateral resolution [13, 89]. Katemann et al. used AC-SECM to characterize the solid–liquid interface of lacquered

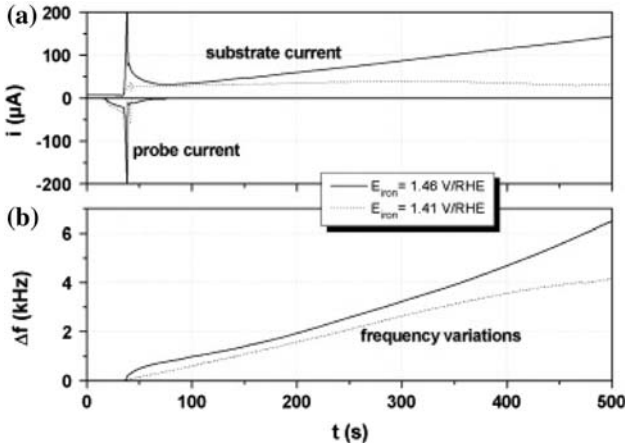

Fig. 7 Simultaneous probe and substrate current variations (**a**) and frequency variations (**b**) recording during the pit initiation and propagation process of iron in 0.01 M KOH as a function of time. Chloride amount: $Q_{AgCl} = 1.2$ mC; tip-to-substrate distance: $z = 75$ μm. The thickness of the iron deposit was 2.5 μm and the resonance microbalance frequency was 9 MHz. Reprinted from [71]. Copyright 2007, Elsevier Science Ltd

tinplates in contact with aqueous solutions [5]. It was shown that AC-SECM has the capability to distinguish between regions on the samples surface with an intact coating and with failures in the protecting polymer film. Furthermore, microscopic domains of a varying conductivity/electrochemical activity on surface artificial microcavities such as cracks and pinholes used as a representative model of precursor sites for localized corrosion were clearly identified and properly visualized at a high spatial resolution.

Summary and outlook

In more recent years, lots of researches have focused on understanding the problem from a surface science perspective to determine the localized chemistry involved in corrosion processes. SECM, as one of a series of promising instrumental methods to recognize the phenomena of localized corrosion, is a coupling of scanning probe techniques with electrochemistry sensitivity. In comparison with other local probe techniques to investigate corrosion processes, SECM has the advantages to in situ characterize both topography and localized corrosion activity of microscopic defects at the metal/passive film/electrolyte interface and, especially, it is good at pursuing the microscopic information occurring at the early stages of localized corrosion.

As pitting corrosion belongs to a random event, it is therefore a difficult task to predict where a pit will occur on the metal surface and how many pits will produce. This renders difficult the use of local probes for studying the early stages of the pit initiation and propagation. To tackle the problem, the advantage of the SECM technique can be taken to generate a single pit on substrate of metals such as iron in various media. The use of the SECM for this purpose allows a locally aggressive chemical environment to be rapidly established at a preselected site on the bulk metal surface to initiate localized corrosion. That is, with the SECM-tip close to the metal surface to be studied, electrolysis allows the solution composition in the gap between the tip and substrate to be changed within a few milliseconds.

Organic coatings are widely used as a protection measure against metal corrosion owing to their function as a physical barrier between the metal substrate and corrosive environment. However, complete isolation of the underlying metal substrate from the environment can not be achievable since all polymers are permeable to corrosive species such as oxygen, water, and ions. Techniques with local resolution are therefore potentially useful for studying the degradation of coated metals. It has been demonstrated that the SECM is a powerful technique for the in situ investigation of both the transport processes that occur through the organic coatings, and the consequent corrosion reactions at the metal/electrolyte interface during their exposure to electrolytes.

As a trend in developing the state-of-the-art of SECM, the combination of SECM with various local techniques, such as EC-STM, EC-AFM, SVET, SRET, SKP, LEIS, NSOM, and even EQCM, have been shown capable to provide more microscopic and comprehensive information on the processes occurring at the surface of corroding metals.

The application range of SECM technique in studying corrosion of metals is likely to expand greatly in the future. Some improvements in the experiment design and operation as well as the foreseeable application range could be proposed, such as: (1) An integrated SECM/SPM to pursue a tremendous improvement of lateral resolution in the nanometer scale; (2) An array of microelectrodes (probes) created by micromachining to increase the time resolution for SECM imaging; (3) Accurate positioning of the probe above a defect (e.g., inclusion, segregation, intermetallic precipitate, etc.); (4) Inhomogeneous corrosion processes at grain boundaries or on individual grains; and (5) SECM characterization of localized corrosion of metals under stress or strain condition in real time.

Acknowledgments This work was supported by the Special Funds for the Major State Basic Research Projects (973 Projects) (Grant No. 2006CB605004) and the Natural Science Foundation of Shandong Province, China (Grant No. Y2006B16).

References

1. Strehblow HH (1995) In: Marcus P, Oudor J (eds) Corrosion mechanisms in theory and practice. Marcel Dekker, New York, p 201

2. Perez N (2004) Electrochemistry and corrosion science. Kluwer, New York
3. de Wit JWH, van der Weijde DH, de Jong A, Blekkenhorst F, Meijers SD (1998) In: Sixth international symposium on electrochemical methods in corrosion research, Pt. 1 and 2, vol 289–292, p 69
4. Frankel GS (1998) J Electrochem Soc 145:2186
5. Katemann BB, Inchauspe CG, Castro PA, Schulte A, Calvo EJ, Schuhmann W (2003) Electrochim Acta 48:1115
6. Gabrielli C, Joiret S, Keddam M, Portail N, Rousseau P, Vivier V (2008) Electrochim Acta 53:7539
7. Oltra R, Maurice V, Akid R, Marcus P (eds) (2007) Local probe techniques for corrosion research. Woodhead, Cambridge
8. Khobaib M, Rensi A, Matakis T, Donley MS (2001) Prog Org Coat 41:266
9. Lu BT, Chen ZK, Luo JL, Patchett BM, Xu ZH (2005) Electrochim Acta 50:1391
10. Krawiec H, Vignal V, Oltra R (2004) Electrochem Commun 6:655
11. Simões AM, Bastos AC, Ferreira MG, González-García Y, González S, Souto RM (2007) Corros Sci 49:726
12. Bastos AC, Zheludkevich ML, Ferreira MGS (2008) Prog Org Coat 63:282
13. Katemann BB, Schulte A, Calvo EJ, Koudelka-Hep M, Schuhmann W (2002) Electrochem Commun 4:134
14. Li MC, Cheng YF (2008) Electrochim Acta 53:2831
15. Sykes JM, Doherty M (2008) Corros Sci 50:2773
16. Suter T, Böhni H (1998) Electrochim Acta 43:2843
17. Engstrom RC, Weber M, Wunder DJ, Burgess R, Winquist S (1986) Anal Chem 58:844
18. Lister TE, Pinhero PJ (2002) Electrochem Solid-State Lett 5:B33
19. Liu H-Y, Fan F-RF, Lin CW, Bard AJ (1986) J Am Chem Soc 108:3838
20. Bard AJ, Fan F-RF, Kwak J, Lev O (1989) Anal Chem 61:132
21. Bard AJ, Fan F-RF, Pierce DT, Unwin PR, Wipf DO, Zhou FM (1991) Science 254:68
22. Tóth K, Nagy G, Wei C, Bard AJ (1995) Electroanalysis 7:801
23. Zhou JF, Zu YB, Bard AJ (2000) J Electroanal Chem 491:22
24. Bi SP, Liu B, Fan FRF, Bard AJ (2005) J Am Chem Soc 127:3690
25. Zhan D, Li X, Zhan W, Fan F-RF, Bard AJ (2007) Anal Chem 79:5225
26. Bard AJ, Fan F-R, Mirkin MV (2001) In: Bard AJ, Mirkin MV (eds) Scanning electrochemical microscopy. Marcel Dekker, New York
27. Wittstock G, Burchardt M, Pust SE, Shen Y, Zhao C (2007) Angew Chem Int Ed 46:1584
28. Niu L, Cao X, Lu M (2007) In: Jiang PN (ed) Electroanalytical chemistry research developments. Nova Science, Hauppauge, pp 1–5
29. González-García Y, Burstein GT, González S, Souto RM (2004) Electrochem Commun 6:637
30. Pistorius PC, Burstein GT (1992) Philos Trans R Soc Lond A 341:531
31. Williams DE, Westcott C, Fleischmann M (1985) J Electrochem Soc 132:1804
32. Frankel GS, Stockert L, Hunkeler F, Bohni H (1987) Corrosion 43:429
33. Bohni H, Stockert L (1989) Mater Sci Forum 44:313
34. Isaacs HS (1989) Corros Sci 29:313
35. Pistorius PC, Burstein GT (1992) Corros Sci 33:1885
36. Stewart J, Balkwill PH, Williams DE (1994) Corros Sci 36:1213
37. Zhu Y, Williams DE (1997) J Electrochem Soc 144:L43
38. Williams DE, Mohiuddin TF, Zhu YY (1998) J Electrochem Soc 145:2664
39. Burstein GT, Vines SP (2001) J Electrochem Soc 148:B504
40. Bastos AC, Simões AM, González S, González-García Y, Souto RM (2004) Electrochem Commun 6:1212
41. Baltes N, Thouin L, Amatore C, Heinze J (2004) Angew Chem Int Ed 43:1431
42. Riley AM, Wells DB, Williams DE (1991) Corros Sci 32:1307
43. Burstein GT, Mattin SP (1992) Philos Mag Lett 66:127
44. Williams DE, Newman RC, Kelly RG, Song Q (1991) Nature 350:216
45. Wranglen G (1969) Corros Sci 9:585
46. Szlarska-Smialowska Z (1972) Corrosion 28:388
47. Eklund GE (1974) J Electrochem Soc 121:467
48. Castle JE, Ke R (1990) Corros Sci 30:409
49. Newman RC (1985) Corros Sci 24:331
50. Ke R, Alkire R (1995) J Electrochem Soc 142:4056
51. Paik CH, White HS, Alkire RC (2000) J Electrochem Soc 147:4120
52. Lister TE, Pinhero PJ (2003) Electrochim Acta 48:2371
53. Bard AJ, Fan FF, Mirkin M (1994) In: Bard AJ (ed) Electroanalytical chemistry, vol 18. Marcel Dekker, New York, p 287
54. Lister TE, Pinhero PJ (2002) Electrochem Solid State Lett 5:B33
55. Völker E, Inchauspe CG, Calvo EJ (2006) Electrochem Commun 8:179
56. Fushimi K, Lill KA, Habazaki H (2007) Electrochim Acta 52:4246
57. Yin YH, Niu L, Lu M, Guo WK, Chen SH (2009) Appl Surf Sci (revised)
58. Serebrennikova I, White HS (2001) J Electrochem Soc 4:B4
59. Casillas N, Charlebois SJ, Smyrl WH, White HS (1993) J Electrochem Soc 140:L142
60. Casillas N, Charlebois SJ, Smyrl WH, White HS (1994) J Electrochem Soc 141:636
61. Basame SB, White HS (1998) J Phys Chem 102:9812
62. Basame SB, White HS (1999) Langmuir 15:819
63. Frichet A, Gimenez P, Keddam M (1993) Electrochim Acta 38:1957
64. Serebrennikova I, Lee S, White HS (2002) Faraday Discuss 121:199
65. Still JW, Wipf DO (1997) J Electrochem Soc 144:2657
66. Fushimi K, Azumi K, Seo M (1999) Proc Electrochem Soc 98-17:626
67. Fushimi K, Seo M (2001) J Electrochem Soc 148:B450
68. Vuillemin B, Philippe X, Oltra R, Vignal V, Coudreuse L, Dufour LC, Finot E (2003) Corros Sci 45:1143
69. Fushimi K, Azumi K, Seo M (2000) J Electrochem Soc 147:552
70. Gabrielli C, Joiret S, Keddam M, Perrot H, Portail N, Rousseau P, Vivier V (2006) J Electrochem Soc 153:b68
71. Gabrielli C, Joiret S, Keddam M, Perrot H, Portail N, Rousseau P, Vivier V (2007) Electrochim Acta 52:7706
72. Shreir LL, Jarman RA, Burstein GT (eds) (1994) Corrosion, vol 2, 3rd edn. Butterworth-Heinemann, Oxford (Chap. 14)
73. Grundmeier G, Simoes A (2003) In: Bard AJ, Stratmann M (eds) Encyclopedia of electrochemistry, vol 4. Wiley-VCH, Weinheim, p 499
74. Souto RM, González-García Y, González S, Burstein GT (2004) Corros Sci 46:2621
75. Bastos AC, Simões AM, González S, González-García Y, Souto RM (2005) Prog Org Coat 53:177
76. Souto RM, González-García Y, González S (2005) Corros Sci 47:3312
77. Souto RM, González-García Y, González S (2008) Corros Sci 50:1637
78. Jones CE, Macpherson JV, Barber ZH, Somekh RE, Unwin PR (1999) Electrochem Commun 1:55
79. Macpherson JV, Unwin PR (2000) Anal Chem 72:276
80. Kranz C, Friedbacher G, Mizaikoff B, Lugstein A, Smolier J, Bertagnolli E (2001) Anal Chem 73:2491

81. Meier J, Friedrich KA, Stimming U (2002) Faraday Discuss 121:365
82. Treutler TH, Wittstock G (2003) Electrochim Acta 48:2923
83. Davoodi A, Pan J, Leygraf C, Norgren S (2005) Electrochem Solid State Lett 8:b21
84. Davoodi A, Pan J, Leygraf C, Norgren S (2007) Electrochim Acta 52:7697
85. Simões A, Battocchi D, Tallman D, Bierwagen G (2008) Prog Org Coat 63:260
86. Büchler M, Kerimo J, Guillaume F, Smyrl WH (2000) J Electrochem Soc 147:3691
87. Knutson TL, Guillaume F, Lee W-J, Alhoshan M, Smyrl WH (2003) Electrochim Acta 48:3229
88. Gabrielli C, Keddam M, Torresi R (1991) J Electrochem Soc 138:2657
89. Horrocks BR, Schmidtke D, Heller A, Bard AJ (1993) Anal Chem 65:3605